Electronic Supplementary Information

Urchin like $Ni_xCo_{3-x}O_4$ hierarchical nanostructures as non-precious, bifunctional electrocatalyst for anion exchange membrane alkaline alcohol fuel cells

Palanisamy Manivasakan, Parthiban Ramasamy and Jinkwon Kim*

Department of Chemistry and GETRC, Kongju National University, 182, Shinkwondong, Kongju, 314-701, Chungnam-do, Republic of Korea

**Corresponding Author*
E-mail: jkim@kongju.ac.kr, Fax: +82-41-850-8613; Tel: +82-41-850-8496.

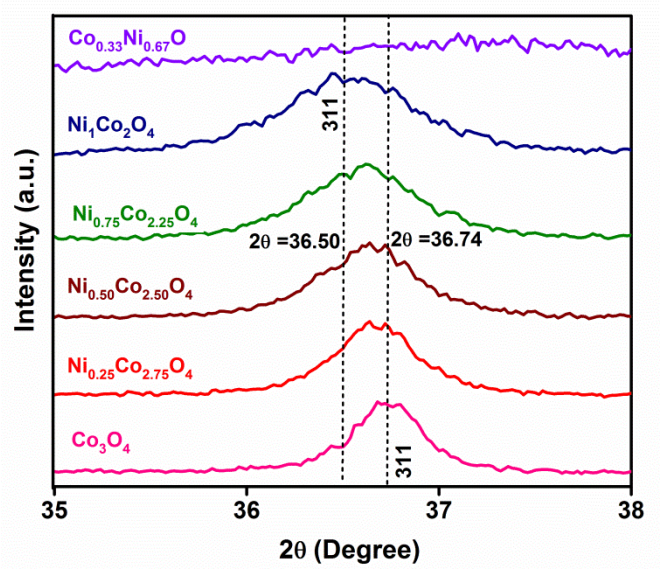

Fig.S1. Expanded (311) XRD peaks of Co_3O_4, $Ni_xCo_{3-x}O_4$ and $Co_{0.33}Ni_{0.67}O$.

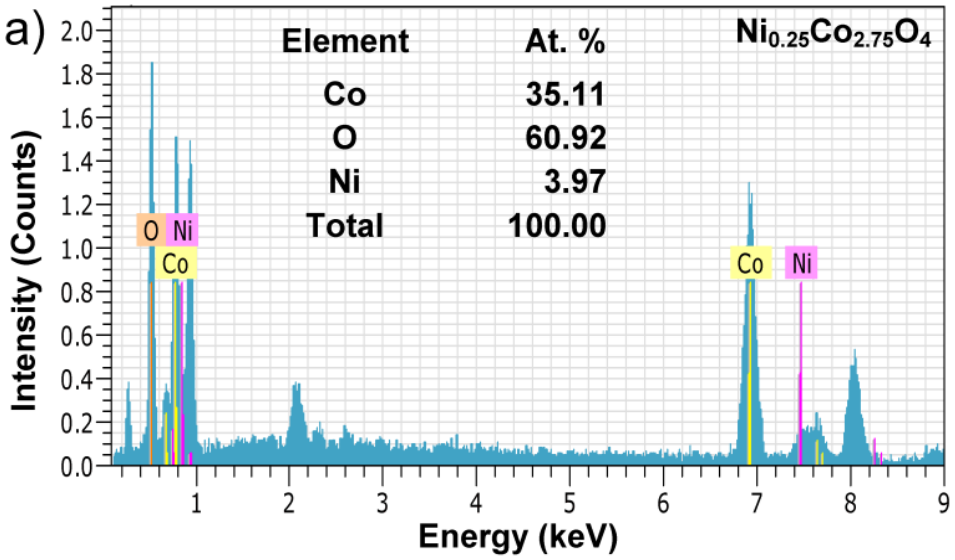
a)
Element
At. %
Co 35.11
O 60.92
Ni 3.97
Total 100.00
Ni0.25Co2.75O4
O
Ni
Co
Co
Ni
Intensity (Counts)
Energy (keV)

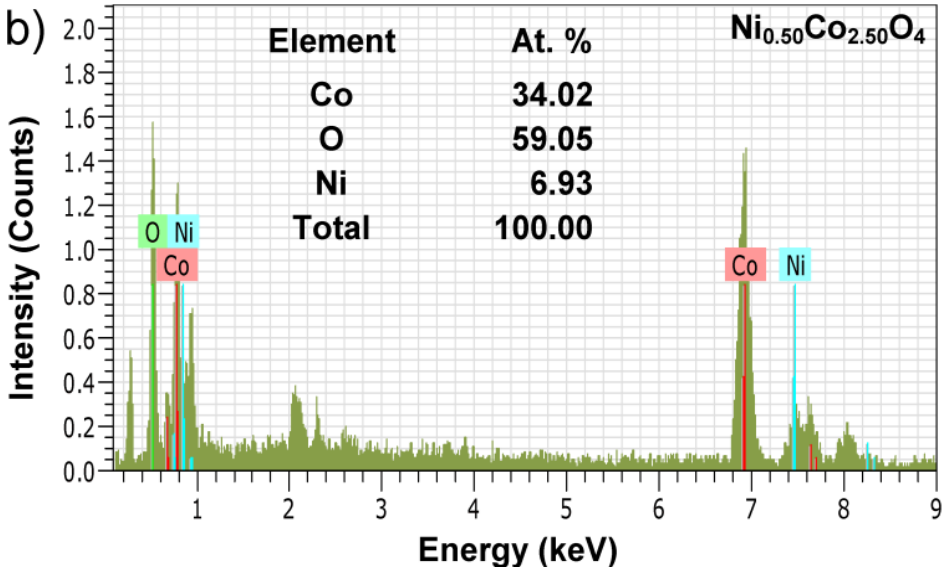
b)
Element
At. %
Co 34.02
O 59.05
Ni 6.93
Total 100.00
Ni0.50Co2.50O4
O
Ni
Co
Co
Ni
Intensity (Counts)
Energy (keV)

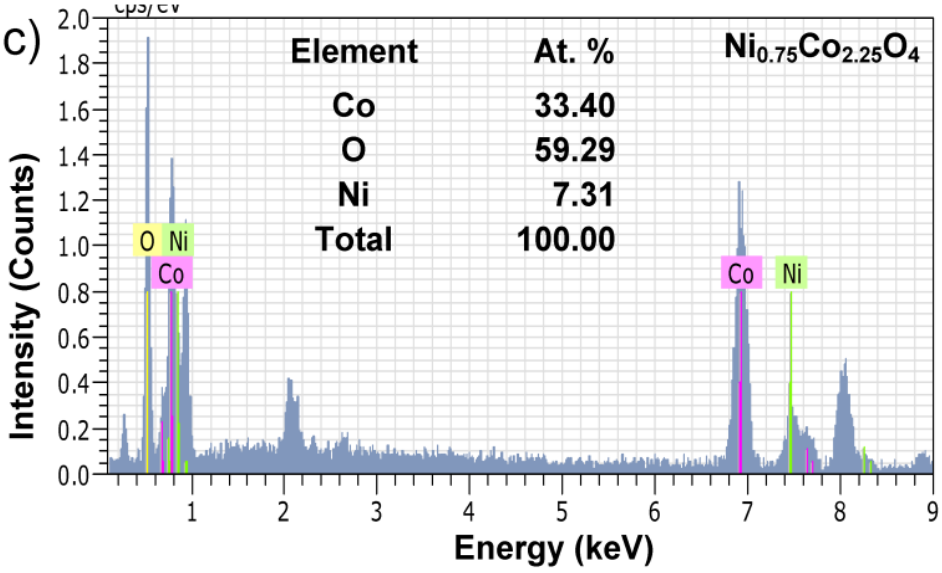
c)
Element
At. %
Co 33.40
O 59.29
Ni 7.31
Total 100.00
Ni0.75Co2.25O4
O
Ni
Co
Co
Ni
Intensity (Counts)
Energy (keV)

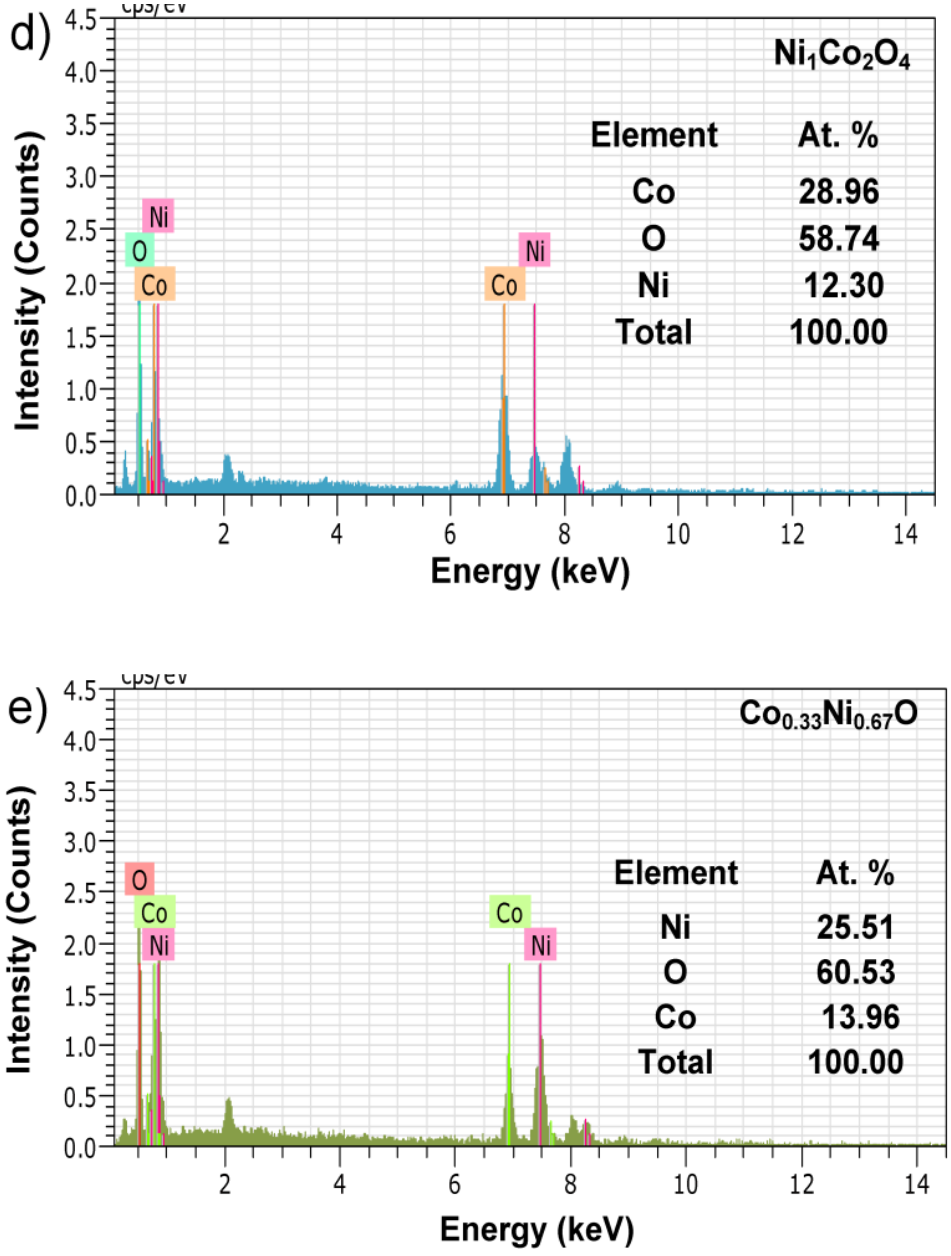

Fig.S2. EDX Profiles of a) $Ni_{0.25}Co_{2.75}O_4$, b) $Ni_{0.50}Co_{2.50}O_4$, c) $Ni_{0.75}Co_{2.25}O_4$, d) $Ni_1Co_2O_4$ and e) $Co_{0.33}Ni_{0.67}O$.

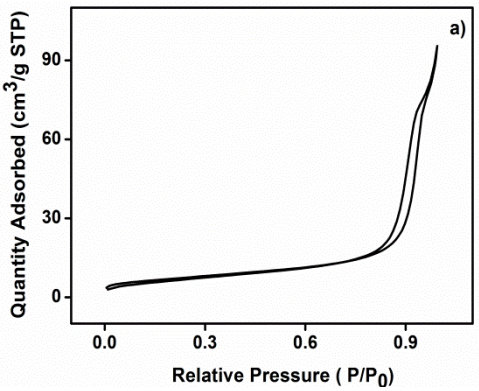
a)
Quantity Adsorbed (cm3/g STP)
90
60
30
0
0.0
0.3
0.6
0.9
Relative Pressure (P/P0)

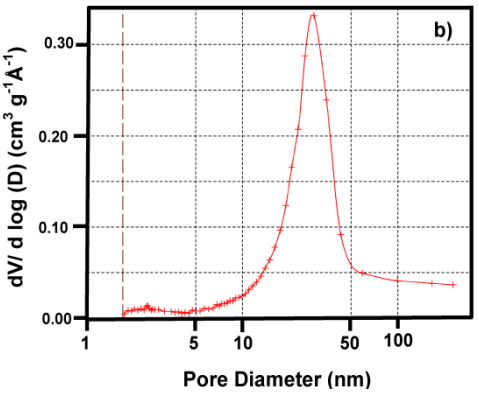
b)
dV/ d log (D) (cm3 g-1Å-1)
0.30
0.20
0.10
0.00
1
5
10
50
100
Pore Diameter (nm)

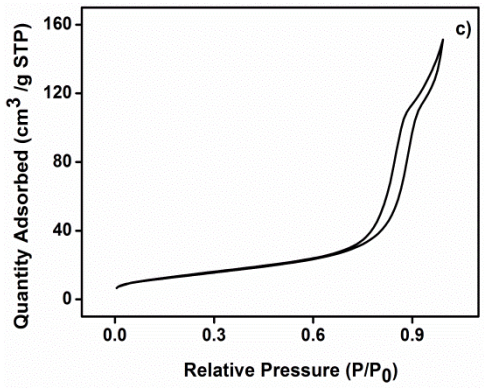
c)
Quantity Adsorbed (cm3 /g STP)
160
120
80
40
0
0.0
0.3
0.6
0.9
Relative Pressure (P/P0)

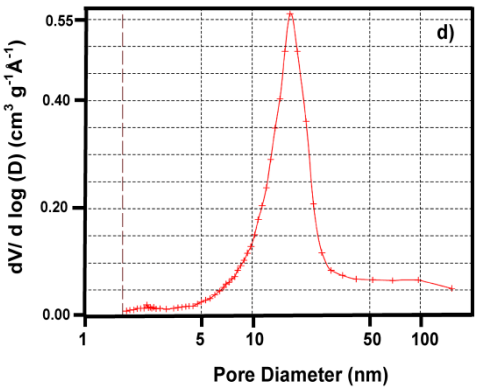
d)
dV/ d log (D) (cm3 g-1Å-1)
0.55
0.40
0.20
0.00
1
5
10
50
100
Pore Diameter (nm)

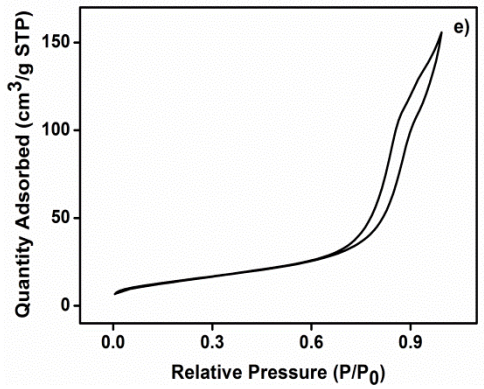
e)
Quantity Adsorbed (cm3/g STP)
150
100
50
0
0.0
0.3
0.6
0.9
Relative Pressure (P/P0)

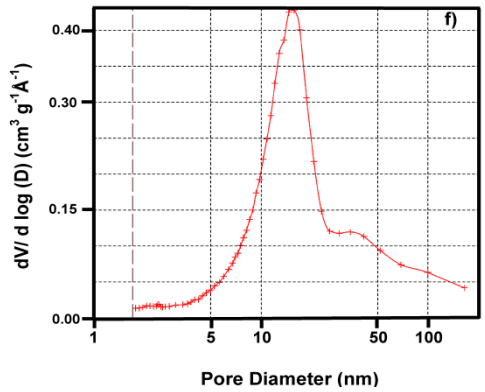
f)
dV/ d log (D) (cm3 g-1Å-1)
0.40
0.30
0.15
0.00
1
5
10
50
100
Pore Diameter (nm)

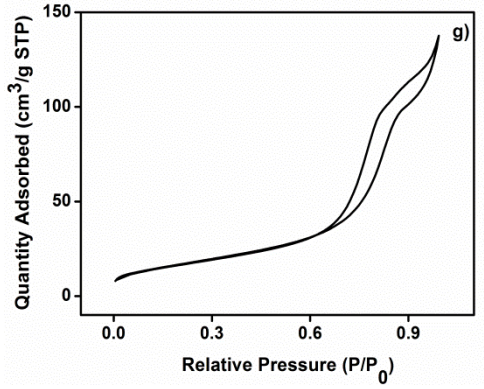
g)
Quantity Adsorbed (cm3/g STP)
150
100
50
0
0.0
0.3
0.6
0.9
Relative Pressure (P/P0)

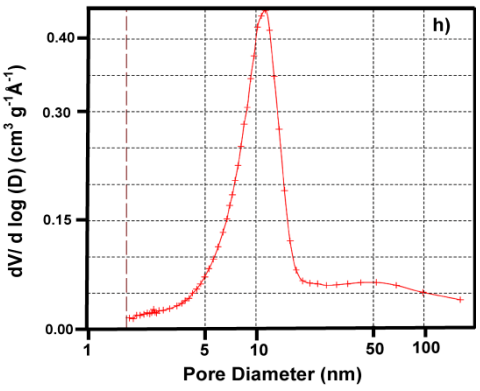
h)
dV/ d log (D) (cm3 g-1Å-1)
0.40
0.30
0.15
0.00
1
5
10
50
100
Pore Diameter (nm)

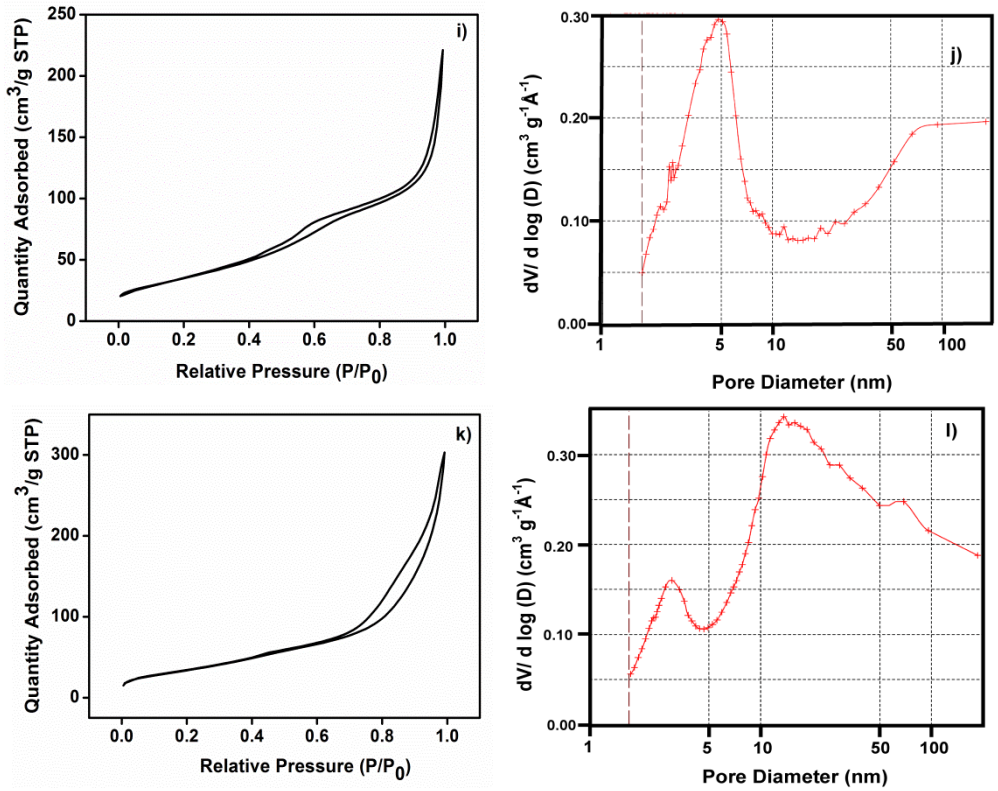

Fig.S3. N_2 adsorption-desorption isotherm and pore size distribution plots of Co_3O_4 (a & b), $Ni_{0.25}Co_{2.75}O_4$ (c & d), $Ni_{0.50}Co_{2.50}O_4$ (e & f), $Ni_{0.75}Co_{2.25}O_4$ (g & h), $Ni_1Co_2O_4$ (i & j) and $Co_{0.33}Ni_{0.67}O$ (k & l) hierarchical nanostructures.

Table S1. Textural data of porous nickel cobaltite 3D hierarchical nanostructures.

3D Hierarchical Nanostructures	**BET Specific Surface Area ($m^2 g^{-1}$)**	**Range of Major Pore Size Distribution ± 2 (nm)**	**BJH Adsorption Cumulative Surface Area of Pores ($m^2 g^{-1}$)**	**Total Pore Volume ($cm^3 g^{-1}$)**	**Average Pore Size (nm)**
Co_3O_4	25.38	10 - 50	26.25	0.15	23.26
$Ni_{0.25}Co_{2.75}O_4$	49.11	07 - 40	60.13	0.23	19.05
$Ni_{0.50}Co_{2.50}O_4$	51.10	05 - 35	66.05	0.24	18.86
$Ni_{0.75}Co_{2.25}O_4$	59.72	03 - 25	79.12	0.25	14.25
$Ni_1Co_2O_4$	122.78	02 - 10	156.20	0.34	11.14
$Co_{0.33}Ni_{0.67}O$	119.80	02 - 05-100	152.76	0.47	15.65

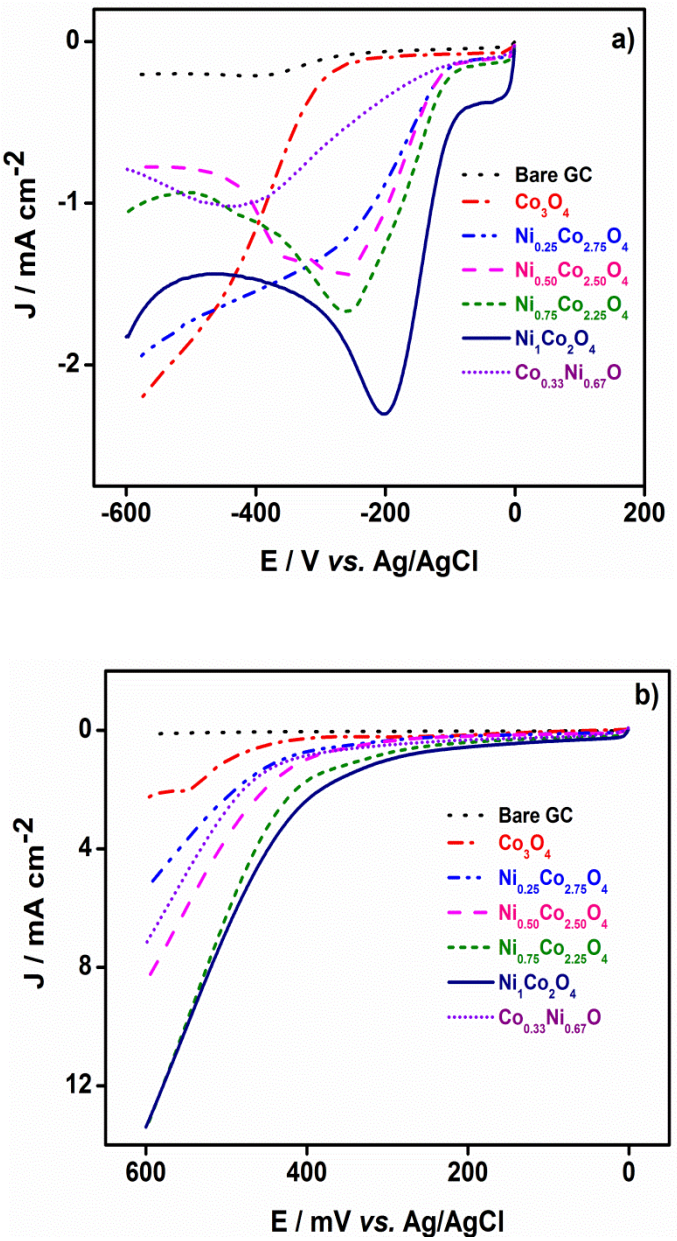

Fig.S4. Linear sweep voltammetry (LSV) curves of a) Oxygen Reduction Reaction (ORR) and b) Methanol Oxidation Reaction (MOR).

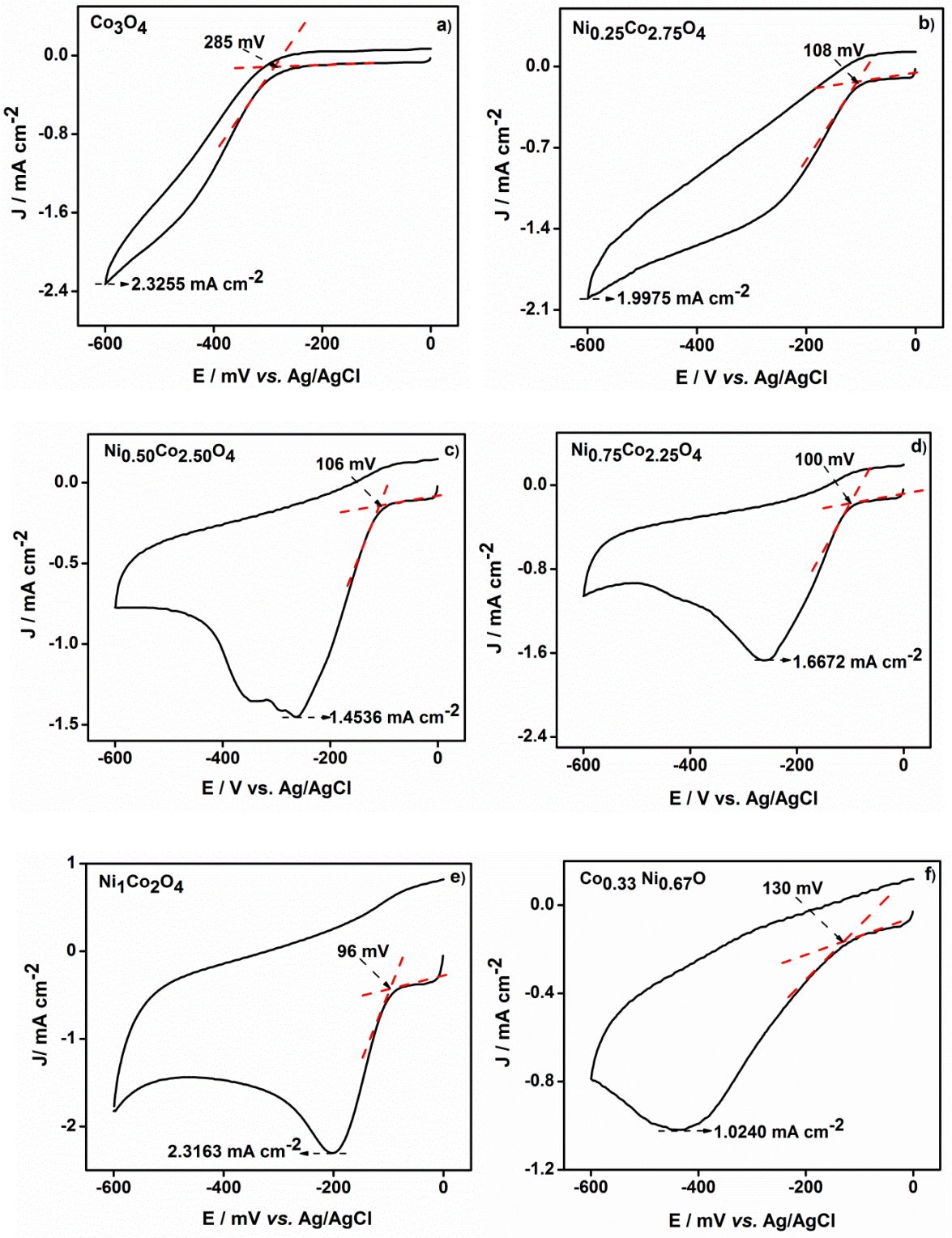

Fig.S5. Current density measurements and onset potential calculations for the ORR a) Co_3O_4, b) $Ni_{0.25}Co_{2.75}O_4$, c) $Ni_{0.50}Co_{2.50}O_4$, d) $Ni_{0.75}Co_{2.25}O_4$, e) $Ni_1Co_2O_4$ and f) $Co_{0.33}Ni_{0.67}O$.

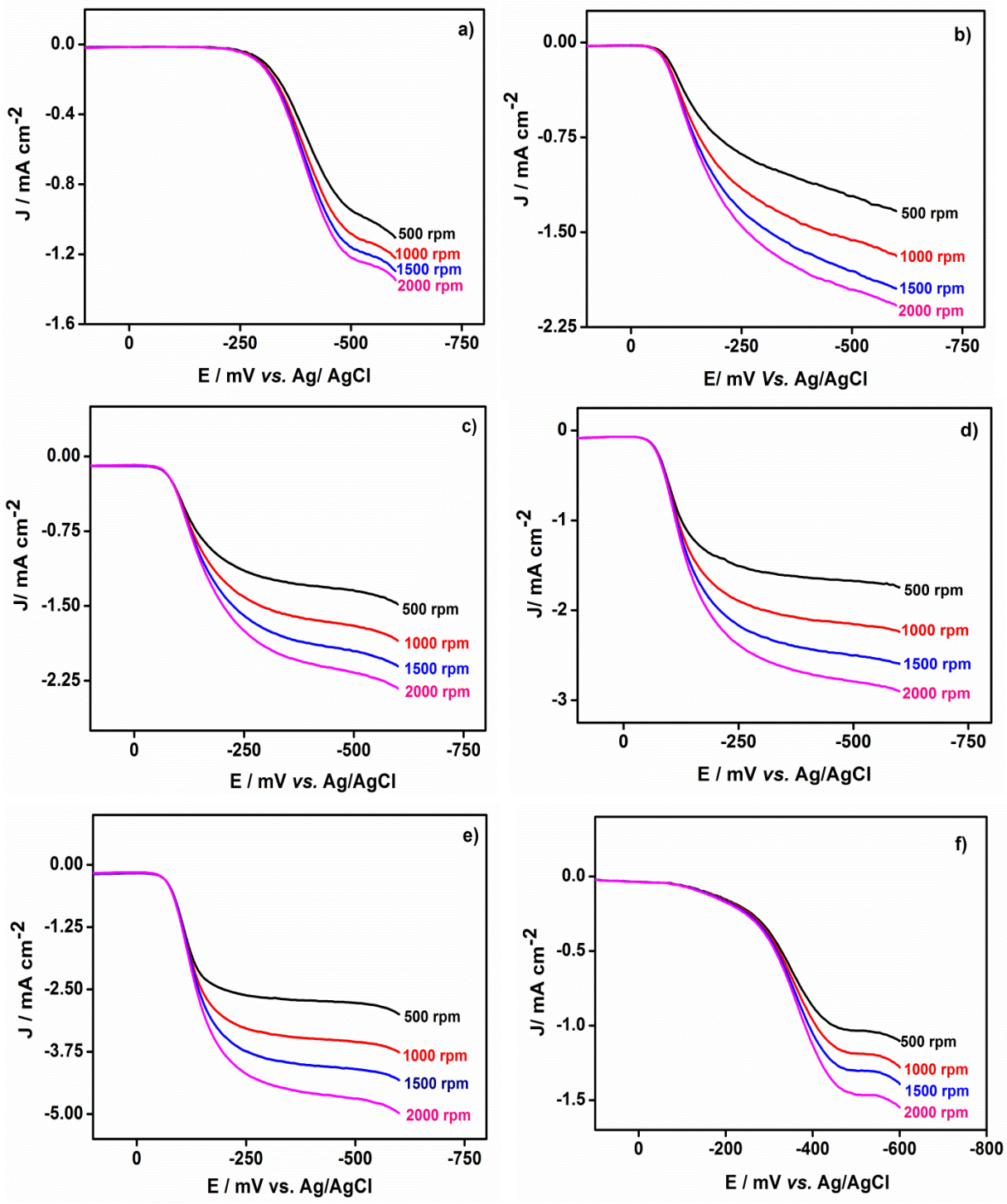

Fig.S6. Linear sweep voltammetry curves of ORR at various rotation rates with a sweep rate of 5 mVs^{-1} at a) Co_3O_4, b) $Ni_{0.25}Co_{2.75}O_4$, c) $Ni_{0.50}Co_{2.50}O_4$, d) $Ni_{0.75}Co_{2.25}O_4$, e) $Ni_1Co_2O_4$ and f) $Co_{0.33}Ni_{0.67}O$.

Rotating-disk voltammograms were recorded on different catalyst-modified electrodes in oxygen saturated 0.1 M KOH solution at different rotation rates (varying rotation speed from 500 rpm to 2000 ± 5 rpm) with a sweep rate of 5 mVs^{-1}. Rotating-disk electrode (RDE) current-potential data can be applied to construct the Koutecky-Levich (*K-L*) curves according to the equations (1) and (2),

$$1/J = 1/J_K + 1/J_L = 1/J_k + 1/B\,\omega^{0.5} \quad (1)$$

$$B = 0.62nF\,C_{O_2}\,(D_{O_2})^{2/3}\,v^{-1/6} \quad (2)$$

where J is the measured current density, J_K and J_L are the kinetic and diffusion limiting current density, respectively, ω is the angular frequency of the rotation (rad s^{-1}), n represents the overall number of electrons transferred during oxygen reduction, F is the Faraday constant (F = 96485 C mol^{-1}), Do_2 is the diffusion coefficient of O_2 in 0.1 M KOH (1.9×10^{-5} cm^2 s^{-1}), υ is the kinetic viscosity (0.01 cm^2 s^{-1}), and Co_2 is the saturated oxygen concentration in 0.1 M KOH (1.2×10^{-6} mol cm^{-3}). The constant 0.62 is adopted when the rotation speed is expressed in rad s^{-1}. A plot of the inverse of the current density J^{-1} *versus* $\omega^{-0.5}$ should yield a straight line with the intercept (J_K) and the slope (B factor). Subsequently, the B factor and the literature data of the other parameters (as mentioned above) have been used to calculate the electron transfer number (n) values according to the Eq.2.

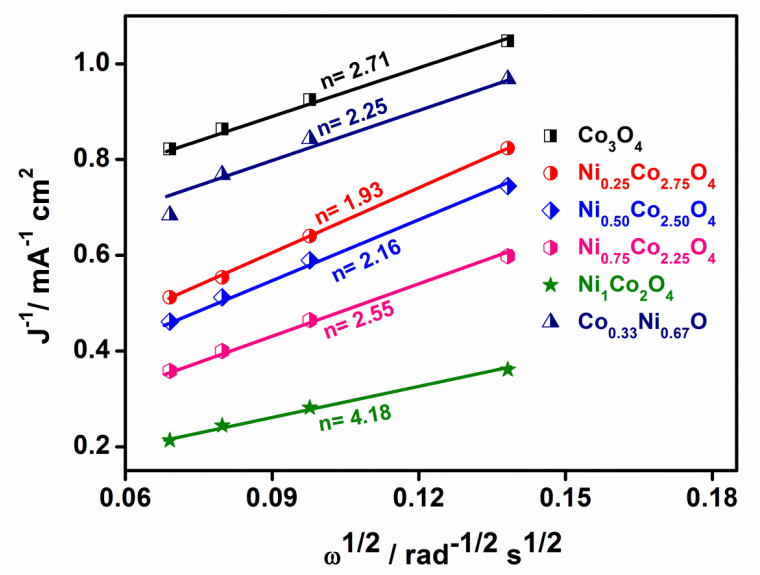

Fig.S7. Koutecky-Levich plots for ORR at -500 mV *vs.* Ag/AgCl.

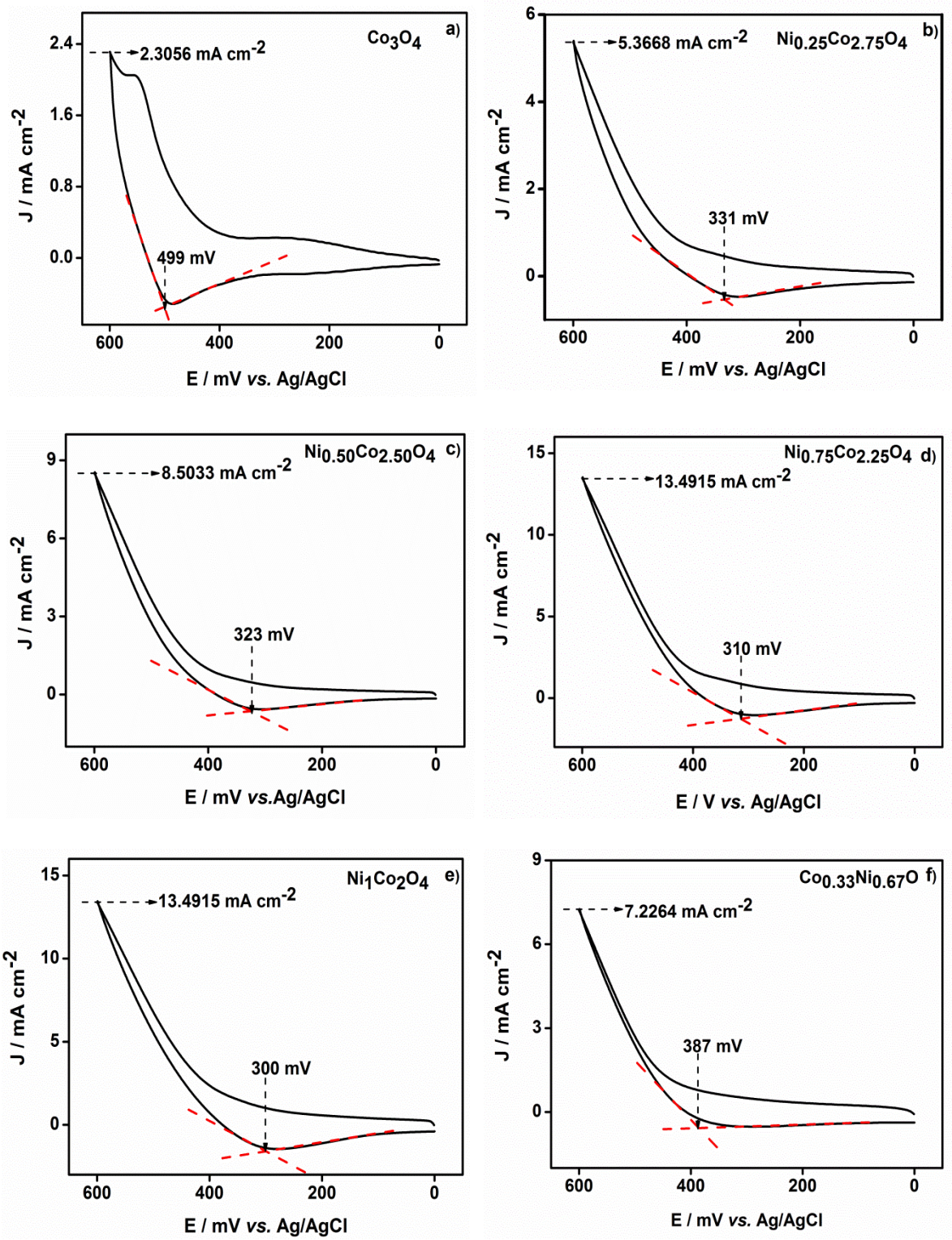

Fig.S8. Current density measurements and onset potential calculations for the MOR a) Co_3O_4, b) $Ni_{0.25}Co_{2.75}O_4$, c) $Ni_{0.50}Co_{2.50}O_4$, d) $Ni_{0.75}Co_{2.25}O_4$, e) $Ni_1Co_2O_4$ and f) $Co_{0.33}Ni_{0.67}O$.